Università di Pisa

Modelling of self-organized InAs quantum dots embedded in an AlGaAs/GaAs heterostructure

P. Coli
Dipartimento di Ingegneria dell'Informazione: Elettronica, Informatica, Telecomunicazioni, Università di Pisa
Giuseppe Iannaccone
Dipartimento di Ingegneria dell'Informazione: Elettronica, Informatica, Telecomunicazioni, Università di Pisa

P. Coli, G. Iannaccone, "*Modelling of self-organized InAs quantum dots embedded in an AlGaAs/GaAs heterostructure*", Nanotechnology, **13**, 3, pp.263-266 (2002).

INSTITUTE OF PHYSICS PUBLISHING NANOTECHNOLOGY
Nanotechnology **13** (2002) 263–266 PII: S0957-4484(02)31403-X

Modelling of self-organized InAs quantum dots embedded in an AlGaAs/GaAs heterostructure

P Coli and G Iannaccone

Dipartimento di Ingegneria dell'Informazione, Università degli studi di Pisa,
Via Diotisalvi 2 I-56122 Pisa, Italy

E-mail: p.coli@iet.unipi.it and g.iannaccone@iet.unipi.it

Received 30 November 2001, in final form 19 March 2002
Published 9 May 2002
Online at stacks.iop.org/Nano/13/263

Abstract
We present results from a detailed simulation of InAs quantum dots embedded in an AlGaAs/GaAs heterostructure with a self-consistent three-dimensional solver of the Poisson–Schrödinger equation based on density functional theory and local density approximation. Single-electron effects in the structure are evaluated by computing the electrochemical potential by means of Slater's transition rule. We have evaluated the effect of strain in the InAs dot on the single-electron charging properties of the system, to assess the importance of including strain in the design of single-electron memories based on self-organized quantum dots.

(Some figures in this article are in colour only in the electronic version)

1. Introduction

Stranski–Krastanov growth enables the fabrication of quantum dots whose size, density, and shape can be controlled with reasonable accuracy through growth temperature, flux ratios, and growth rates. In addition, the quantum dots obtained exhibit clean electronic and optical properties as a result of the strong quantum confinement in three dimensions.

Here, we are mainly interested in the single-electron properties of InAs dots, for assessing the possibility of using layers of self-organized quantum dots as a storage medium for non-volatile memory applications. Recent experiments on the AlGaAs/GaAs material system have shown preliminary, but interesting prospects for such applications [1–5].

A high-electron-mobility transistor (HEMT) with a layer of self-organized dots embedded between the gate and the two-dimensional electron gas can store information represented by the threshold voltage shift of the HEMT caused by the charge trapped in the dots. These memories are programmed by applying to the gate a positive voltage of a few volts that lowers the thin high-gap-material conduction band and enhances tunnelling of electrons from the channel to the dots. The small amount of charge involved in the program operation would allow for low power consumption, and short write–erase times.

In order to determine the most promising structures on the basis of physical simulations, we have developed a three-dimensional Poisson–Schrödinger solver [6] based on density functional theory and the local density approximation (DFT-LDA), with the focus on single-electron charging of the dots, rather than on optical properties.

2. Model

In order to reduce the computational resources required we consider a simplified situation in which we have a regular two-dimensional array of InAs dots embedded in an $Al_{0.2}Ga_{0.8}As$ layer as shown in figure 1(*a*). In this way, we can focus on a simulation domain containing only one dot, and enforce periodic boundary conditions by setting to zero the component of the electric field orthogonal to the lateral faces of the simulation domain. As we can see in figure 1(*b*), the simulation domain contains a single lens-shaped InAs dot embedded in a 20 nm layer of $Al_{0.2}Ga_{0.8}As$. The layer structure consists of a GaAs substrate with unintentional acceptor concentration of 10^{15} cm^{-3}, a 20 nm layer of $Al_{0.2}Ga_{0.8}As$ in which a lens-shaped InAs dot is embedded (with a height of 2 nm and a base diameter of 20 nm), an n-doped 40 nm layer of $Al_{0.2}Ga_{0.8}As$, and finally a 10 nm GaAs cap layer. A metal gate is evaporated onto the top surface. The substrate is grounded.

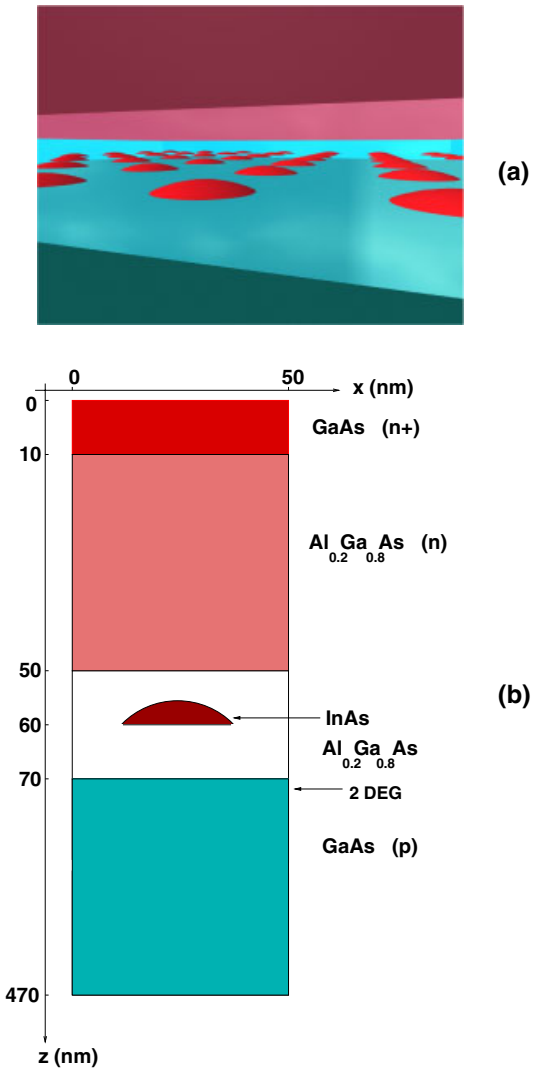

Figure 1. (*a*) The AlGaAs/GaAs heterostructure considered with a regular 2D array of InAs quantum dots; (*b*) the simulation domain containing only one dot.

We have performed a detailed simulation based on the self-consistent solution of the Poisson–Schrödinger equation on a three-dimensional grid with the DFT-LDA: the Poisson–Schrödinger equation is discretized with the box-integration method [7] and solved with the Newton–Raphson algorithm [8].

The potential profile in our domain is determined by the Poisson equation:

$$\nabla \cdot (\epsilon \nabla \phi) = -\rho, \tag{1}$$

where ϕ is the scalar potential, ϵ the dielectric constant, and ρ the charge density, which is given by the following expression:

$$\rho(\boldsymbol{r}) = q[p(\boldsymbol{r}) - n(\boldsymbol{r}) + N_D^+(\boldsymbol{r}) - N_A^-(\boldsymbol{r})] \tag{2}$$

where p and n are the hole and electron densities, N_D^+ and N_A^- are the concentrations of the ionized donors and acceptors, respectively, whose expressions are given, for example, in [9]. While the electron and hole concentrations in the substrate are computed with the semiclassical approximation [9], electrons in the dot are strongly confined, and therefore their density must be computed by solving the Schrödinger equation with the DFT:

$$\left[-\frac{\hbar^2}{2}\nabla \cdot \left(\frac{1}{m}\nabla\right) + V(\boldsymbol{r})\right]\Psi(\boldsymbol{r}) = E\Psi(\boldsymbol{r}), \tag{3}$$

where the potential term is $V(\boldsymbol{r}) = E_c(\boldsymbol{r}) + V_{ex}(\boldsymbol{r})$, m is the effective mass, E_c is the conduction band ($E_c(\boldsymbol{r}) = E_c(\boldsymbol{r} = 0) - q\phi(\boldsymbol{r})$), and V_{ex} is the exchange–correlation potential in the LDA [10]:

$$V_{ex}(\boldsymbol{r}) = -\frac{q^2}{4\pi^2\epsilon_0\epsilon_r}(3\pi^3 n(\boldsymbol{r}))^{1/3}. \tag{4}$$

Once the single-particle eigenfunctions Ψ_i and the corresponding eigenvalues E_i are obtained, the electron density corresponding to a given number N of electrons in the dot can be readily obtained as

$$n(\boldsymbol{r}) = \begin{cases} \displaystyle\sum_{i=1}^{N/2} 2|\Psi_i(\boldsymbol{r})|^2, & \text{if } N \text{ is even} \\ \displaystyle\sum_{i=1}^{(N-1)/2} 2|\Psi_i(\boldsymbol{r})|^2 + |\Psi_{[(N+1)/2]}(\boldsymbol{r})|^2, & \text{if } N \text{ is odd} \end{cases} \tag{5}$$

under the assumption that the electron density in the dot is not appreciably different from that in the ground state. We have implemented a self-consistent algorithm: after we solve the Schrödinger equation we put the quantum expression for the electron density in the dot into the Poisson equation, while we use a semiclassical expression in the rest of the domain. The non-linear Poisson equation is then solved with the Newton–Raphson algorithm. The potential profile obtained is then used to solve the Schrödinger equation again in the quantum domain. This is repeated until the two-norm of the difference between two consecutive solutions for the potential at the end of each complete Newton–Raphson scheme is smaller than 25 μV $\times$ number of grid points.

3. Results

In figure 2 we show the single-electron eigenfunctions obtained from the solution of the Schrödinger equation. In particular, figure 2(*a*) is an isosurface plot of the first eigenfunction for $|\Psi_1(r)|^2 = 3 \times 10^{23}$ m^{-3}; figures 2(*b*) and (*c*) show the second and third eigenfunctions for $|\Psi(r)|^2 = 4 \times 10^{24}$ m^{-3}. The light grey area is the confining dot. Because of the symmetry of the dot, we observe that the second and third eigenfunctions are degenerate and have the same shape rotated by 90°.

In figure 3 we show the isosurface plot of the electron density in the dot and in the two-dimensional electron gas ($n = 10^{17}$ cm^{-3}) for nine electrons in the dot and an applied voltage of -1.5 V on the top gate.

As can be seen, the charge in the dot shields the electric field and reduces the electron density in a region below the dot (the hole in the picture). In figure 4 the same electron density in the y–z plane is shown for $x = 25$ nm.

In figure 5 we plot the conduction band profile on the y–z plane for $x = 25$ nm, with an applied gate voltage of -1.5 V

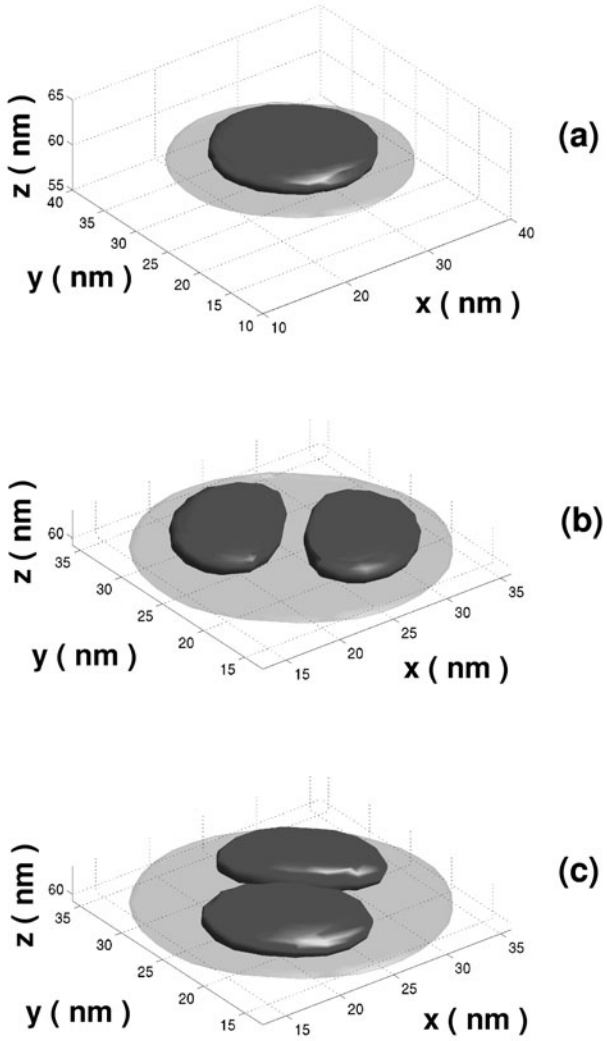

Figure 2. Isosurface plots of the first three eigenfunctions: (*a*) first eigenfunction; (*b*), (*c*) two eigenfunctions related to the second and third degenerate eigenvalues.

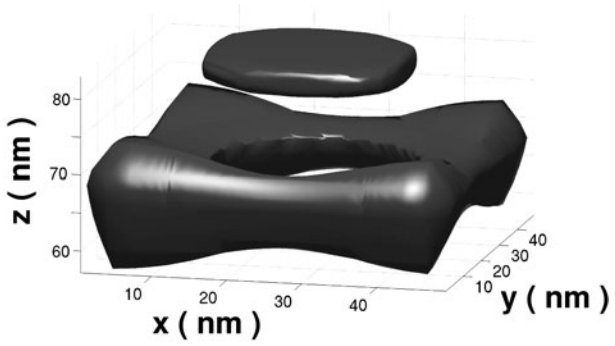

Figure 3. An isosurface plot of the electron density in the dot and in the bottom channel ($n = 10^{17}$ cm^{-3}). The voltage applied to the top gate is $V_g = -1.5$ V and the number of electrons in the dot is nine.

and with nine electrons in the dot: the quantum dot causes a confining potential about 1 eV deep, arising from the difference in electron affinity between the InAs dot and the $Al_{0.2}Ga_{0.8}As$ layer.

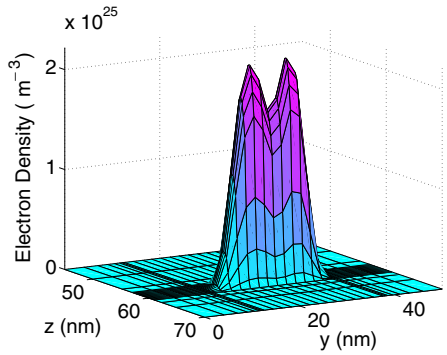

Figure 4. A surface plot of the electron density on a y–z plane passing through the centre of the dot ($x = 25$ nm), with nine electrons in the dot.

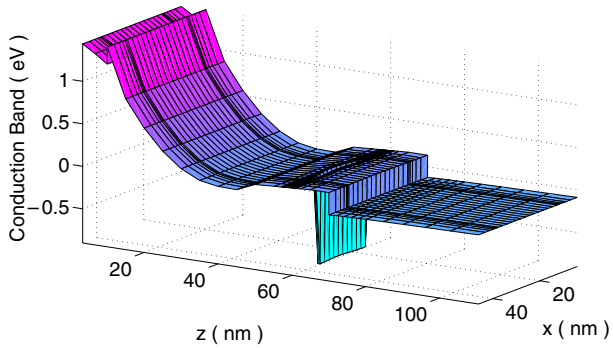

Figure 5. A surface plot of the conduction band on a y–z cross-plane, with nine electron in the dot; $V_g = -1.5$ V. The step in the conduction band of about 0.6 eV defines the quantum confined region.

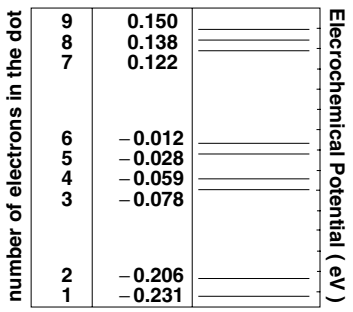

Figure 6. The electrochemical potential for 1–9 electrons in the dot: the plot shows the odd–even pairing.

As far as the charging energies are concerned, in figure 6 we show the electrochemical potential as a function of the number of electrons in the InAs dot. The electrochemical potential is computed with Slater's transition rule as $\mu(N) = E_{N-1/2}$, where $E_{N-1/2}$ is the highest occupied eigenvalue of the system with $N - 1/2$ electrons, computed with DFT. The plot shows the electrochemical potential computed with 1–9 electrons in the dot. The odd–even pairing of the energies of each electron can be noted; from this plot we can see that the charging energy is close to 20 meV, corresponding to a capacitance of 4 aF, and the energy due to quantum confinement is about 150 meV. Figure 7, in contrast, shows how the conduction band increases for the number of electrons in the dot ranging from 1 to 9.

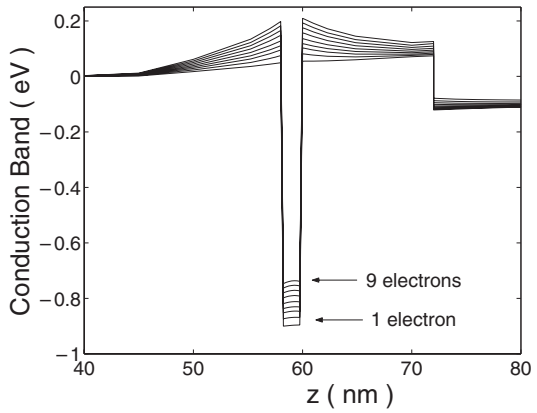

Figure 7. The conduction band for increasing numbers of electrons in the dot (from 1 to 9).

3.1. Strain effects

Self-assembled InAs dots present significant lattice mismatch that causes a high degree of strain. It is therefore important to quantitatively evaluate its effect on the electrical characteristics of the dot. On the basis of previous studies on the strain component in heterostructures in the presence of InAs dots [11–13], we have devised a simplified approach. If we consider the results obtained by the cited studies for the strain tensor with both the continuum elasticity and atomistic valence force field approach [12], we can observe that the hydrostatic component of the strain in the dot is almost constant with a value between 7 and 9%. In our work we want to overestimate the effects of strain and have considered a value of 10% for the hydrostatic component, while for the points outside the dot we have considered zero strain, consistently with the above-mentioned papers. With this approximation, we have added to the potential energy in the Schrödinger equation a term that takes into account the effect of strain in the dot. In particular we have

$$E_c(\boldsymbol{r}) = E_c(\boldsymbol{r})^0 + a_c(\boldsymbol{r})\,\mathrm{Tr}[\epsilon(\boldsymbol{r})] \tag{6}$$

where $E_c(\boldsymbol{r})^0$ is the conduction band without strain, a_c is the deformation potential of the material under hydrostatic deformation, and $\epsilon(\boldsymbol{r})$ is the position-dependent strain tensor. For the conduction band we have considered only the hydrostatic component of the strain. The result is shown in figure 8, where both the conduction band and the single-particle eigenvalues with and without strain are shown on the same plot: we can note that the models considered for the strain produce a translation of the energies of about 0.6 eV.

4. Conclusions

We have presented a program for the three-dimensional simulation of the single-electron properties of self-assembled InAs dots in an AlGaAs/GaAs heterostructure. Our purpose-built Poisson–Schrödinger solver enables us to compute the electronic structure of quantum dots and their electrochemical potential, and is a powerful tool for tuning the layer structure in order to optimize the electric properties of the quantum dot layer for non-volatile memory applications. The approach presented here basically has two important limitations: the treatment of strain is very approximate and the effective-mass approach is too crude an approximation for nanometre-size InAs dots. A detailed approach, based on the *ab initio* calculation of the complete band structure in the strained system, would be required for reproducing the optical properties of the dots, but would have a much smaller impact as regards their electrical properties. In addition, a very complex and accurate model could be deemed excessive, given the present lack of knowledge of experimental parameters such as the exact size, shape, and position for the dots. A systematic investigation aimed at the computer-aided design of non-volatile memory structures in the AlGaAs/GaAs material system, based on the code presented in this paper, is currently in progress.

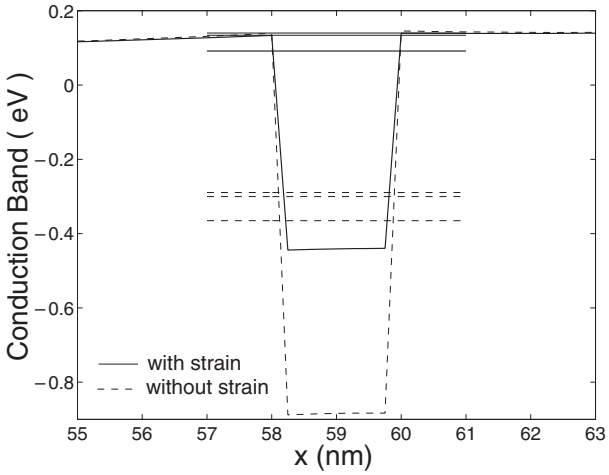

Figure 8. The conduction band and single-particle eigenvalues for the dot obtained considering strain effects (solid lines) and with no strain (dashed lines). The deformation potential is $a_c = -5$ eV, and the hydrostatic component of strain in the dot is 10%.

Acknowledgments

We gratefully acknowledge support from the EU-IST project NANOTCAD (NANO Technology Computer Aided Design IST-1999-10828).

References

[1] Koike K, Saitoh K, Li S, Sasa S, Inoue M and Yano M 2000 *Appl. Phys. Lett.* **76** 1464
[2] Shields A J, O'Sullivan M P, Farrer I, Ritchie D A, Cooper K, Foden C L and Pepper M 1999 *Appl. Phys. Lett.* **74** 735
[3] Phillips J, Kamath K, Brock T and Bhattacharya P 1998 *Appl. Phys. Lett.* **72** 3509
[4] Fonseca L R C, Jimenez J L, Leburton J P and Martin R M 1998 *Phys. Rev.* **57** 4017
[5] Iannaccone G and Coli P 2001 *Appl. Phys. Lett.* **78** 2046
[6] Kumar A, Laux S E and Stern F 1990 *Phys. Rev.* B **42** 5166
[7] Selberherr S *Analysis and Simulation of Semiconductor Devices* (New York: Springer) p 160
[8] Trellakis A, Galick A T, Pacelli A and Ravaioli U 1997 *J. Appl. Phys.* **81**
[9] Sze S 1981 *Physics of Semiconductor Devices* (New York: Wiley) p 23
[10] Inkson 1986 *Many Body Theory of Solids—an Introduction* (New York: Plenum) 15–23
[11] Pryor C 1999 *Phys. Rev.* B **60** 2869
[12] Pryor C, Kim J, Wang L W, Williamson A J and Zunger A 1998 *J. Appl. Phys.* **83** 2548
[13] Cusack M A, Briddon P R and Jaros M 1996 *Phys. Rev.* B **54** 2300